A 3D rigid Mn-MOF heterogeneous catalyst for thioether oxidation, cyanosilylation and Knoevenagel condensation

Han-Fu Liu,[a,b] Zhi-Rong Hu,[b] Tai-Xue Wu,[b] Hong-Mei Hao,[c] Hai-Ye Li,[*b] Fu-Ping Huang[*b]

Table S1 Crystal data and structure refinement for Compound **1**

Identification code	**1**
Empirical formula	$C_{18}H_{14}Mn_2N_8O_4$
Formula weight	516.25
Crystal system	trigonal
Space group	$R\bar{3}$
a/Å	21.6779(8)
b/Å	21.6779(8)
c/Å	12.6682(5)
α/°	90
β/°	90
γ/°	120
Volume/Å^3	5155.6(4)
Z	9
ρ_{calc}g/cm^3	1.496
μ/mm^{-1}	1.142
F(000)	2340.0
Radiation	MoKα (λ = 0.71073)
2Θ range for data collection/°	6.51 to 57.518
Index ranges	$-28 \le h \le 24$, $-27 \le k \le 27$, $-16 \le l \le 14$
Reflections collected	8753
Independent reflections	2713
R_{int}	0.0459
Goodness-of-fit on F^2	1.064
Final R indexes [I>=2σ (I)]	R_1 = 0.0502, wR_2 = 0.1178
Final R indexes [all data]	R_1 = 0.0769, wR_2 = 0.1325

a College of Pharmacy, Guilin Medical University, Guilin 541004, P. R. China.
b State Key Laboratory for the Chemistry and Molecular Engineering of Medicinal Resources, School of Chemistry and Pharmaceutical Sciences, Guangxi Normal University, Guilin 541004, P. R. China.
c Department of Chemistry and Pharmacy, Guilin Normal College，Guilin 541004, P. R. China.
Corresponding author: lihaiye2010@163.com (H.-Y. Li); huangfp2010@163.com (F.-P. Huang).
Electronic Supplementary Information (ESI) available: CCDC 2381922. For ESI and crystallographic data in CIF or other electronic format see DOI: 10.1039/x0xx00000x

Table S2 Selected Bond Lengths (Å) and Angles (°) for Compound **1**

Bond Lengths (Å)			
Mn1—O1A	2.112 (3)	Mn1—N2	2.219 (2)
Mn1—O2	2.125 (3)	Mn1—N3B	2.293 (2)
Mn1—N1	2.355 (3)	Mn1—N4C	2.432 (3)
Bond Angles (°)			
O1A—Mn1—O2	95.68 (12)	O2—Mn1—N3B	95.29 (10)
O1A—Mn1—N1	160.60 (11)	O2—Mn1—N4C	169.41 (10)
O1A—Mn1—N2	89.14 (11)	N1—Mn1—N4C	89.20 (9)
O1A—Mn1—N3B	86.88 (11)	N2—Mn1—N1	72.92 (9)
O1A—Mn1—N4C	87.56 (10)	N2—Mn1—N3B	175.35 (9)
O2—Mn1—N1	90.98 (11)	N2—Mn1—N4C	102.67 (9)
O2—Mn1—N2	87.49 (10)	N3B—Mn1—N1	110.67 (9)
N3B—Mn1—N4C	74.77 (9)		

Symmetry codes: (A) *y*+1/3, -*x*+*y*+2/3, -*z*+2/3; (B) *x*-*y*+1/3, *x*-1/3, -*z*+2/3; (C) -*x*+*y*+1/3, -*x*+2/3, *z*-1/3; (D) -*x*+1, -*y*+1, -*z*+1; (E) -*y*+2/3, *x*-*y*+1/3, *z*+1/3.

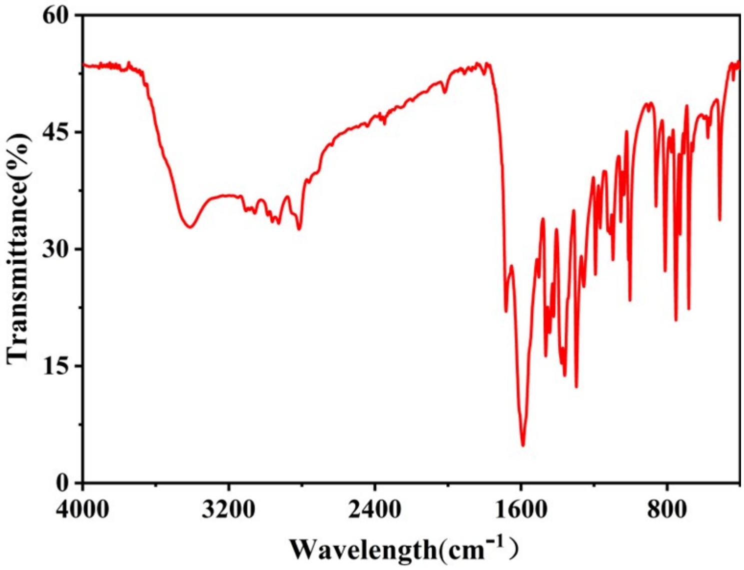

Fig. S1. IR spectra of Compound **1**

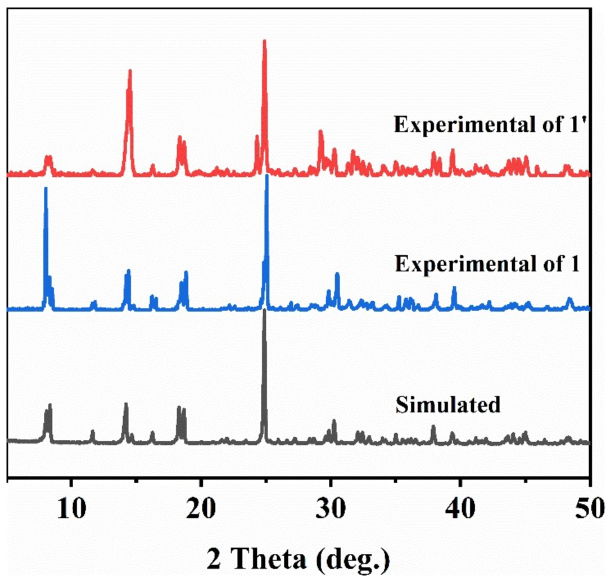

Fig. S2. PXRD patterns of **1** and **1'**

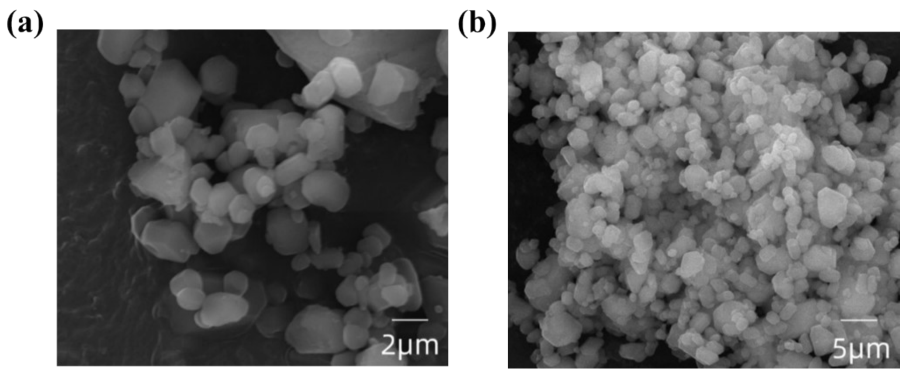

Fig. S3. SEM images of **1'**

Table S3 SHAPE analysis of Mn(II) ion in **1**.

	MnN_4O_2
Coordination modes	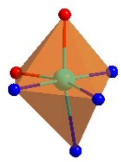
label	OC-6
symmetry	Oh
shape	Octahedron
Calculation results	Distortion(τ_{min}) Mn1（2.311）

Table S4 Optimizing the reaction condition of thioether oxidation catalyzed by $[Mn_2(b\text{-}6\text{-}mpbt)\ (HCOO)_2]_n$.

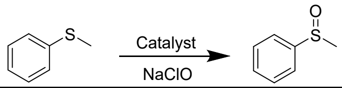

Entry	Thioanisole (mmol)	NaClO (mmol)	$[Mn_2(b\text{-}6\text{-}mpbt)\ (HCOO)_2]_n$ (mg)	Time (h)	T (°C)	Solvent	Conv.[a] (%)
1	4.0	8	40[b]	4	60	DMF	Trace
2	4.0	8	40[b]	4	60	H_2O	16.53
3	4.0	8	40[b]	4	60	EtOH	80.25
4	4.0	8	40[b]	4	60	MeOH	83.34
5	4.0	8	None	4	60	MeOH	9.85
6	4.0	8	10	4	60	MeOH	55.69
7	4.0	8	20	4	60	MeOH	83.25
8	4.0	8	30	4	60	MeOH	92.67
9	4.0	8	40	4	60	MeOH	99.29
10	4.0	8	40	4	50	MeOH	85.54
11	4.0	8	40	4	40	MeOH	62.61
12	4.0	8	40	4	30	MeOH	24.34
13	4.0	8	40	1	60	MeOH	35.83
14	4.0	8	40	2	60	MeOH	62.01
15	4.0	8	40	3	60	MeOH	86.11
16	4.0	4	20	24	60	MeOH	99.32
17	4.0	4	10	24	60	MeOH	93.25
18	4.0	4	5	24	60	MeOH	81.33

a GC-MS measurement was used to determine the conversion rate
b **1** was used as the catalyst.

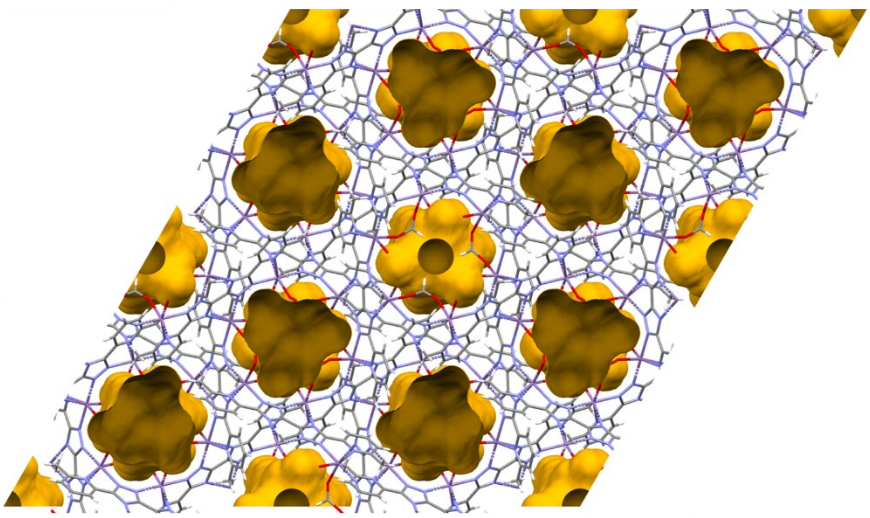

Fig. S4. 3D porous framework of **1**

Table. S5 The catalytic efficiency of different MOFs for thioether oxidation, cyanosilylation and Knoevenagel condensation.

Catalyst	catalytic reaction types	Yield (%)	Ref.
$\{[Mn_2(b\text{-}6\text{-}mpbt)(HCOO)_2]\cdot 1.5CH_3OH\}_n$	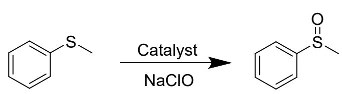	99.29%	This work

UiO-66	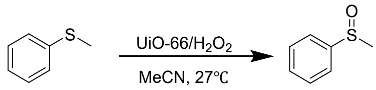	59%	1
UiO-67	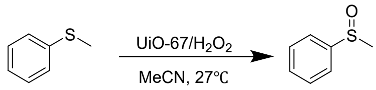	51%	1
$PPh_4[^{SO}{}_2LVO_2]$	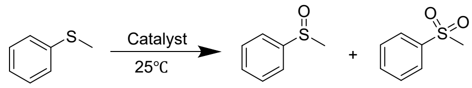	95%	2
$[(TPY\text{-}Br)CuCl(DMSO)(H_2O)]_2$ $[(TPY\text{-}Br)CuCl]_2$ $[W_{10}O_{32}]$ • 2DMSO • $4H_2O$	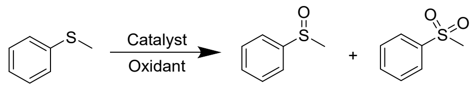	99.9%	3
$(Hbiz)_{12}[(P_2Co_2Mo^V{}_4O_8)_2(P_2Mo^V{}_2O_8)_4$	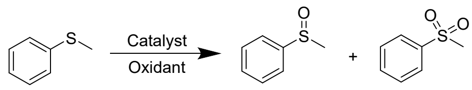	＞99%	4
$(Bu_4N)_4[PW_{11}Nb(O_2)O_{39}]$	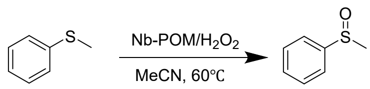	91%	5
$\{[Mn_2(b\text{-}6\text{-}mpbt)(HCOO)_2]\cdot1.5CH_3OH\}_n$	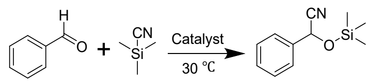	99.16%	This work
Complex 2a	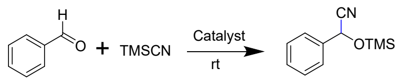	99%	6
Ce-4L	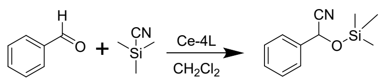	68%	7
$\{(dpdo)[Pr_2(H_2O)_9(dpdo)][Pr(H_2O)_5]_2[Pr(H_2O)_4]_2[V_{10}O_{28}][NiV_{12}O_{38}]$ • $27H_2O\}$	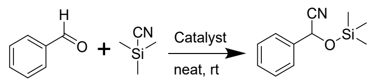	99.6%	8
Y/Eu-MOF	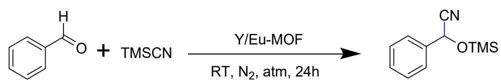	＞99%	9
$\{[Zn_2(4\text{-}tpom)_2(oxdz)_2]$ • $4H_2O\}_n$	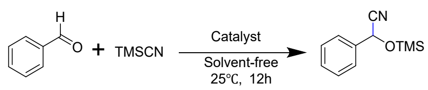	96%	10
Cu(D-Valmet) • xH_2O; $x<1$	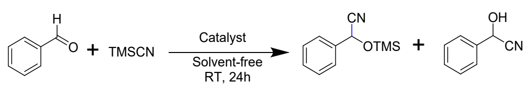	97.3%	11
$\{[Mn_2(b\text{-}6\text{-}mpbt)(HCOO)_2]\cdot1.5CH_3OH\}_n$	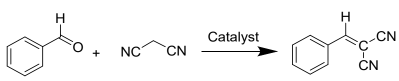	97.37%	This work
Fe_3O_4/cellulose/Co-MOF	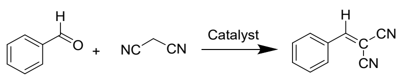	94%	12

MOF-5	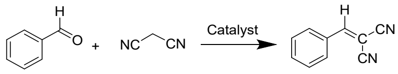	99%	13
Tb-DCBA	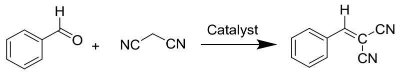	>99%	14
JLU-MOF116	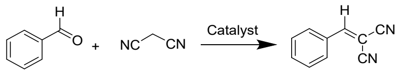	95%	15
JLU-MOF117	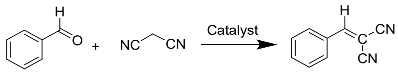	99%	15
Ce-4L	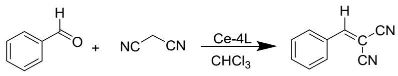	77%	7
{[$Co_3(TNBTB)_2(PTP)$]·7DMF·6 H_2O}$_n$	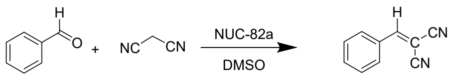	99%	16

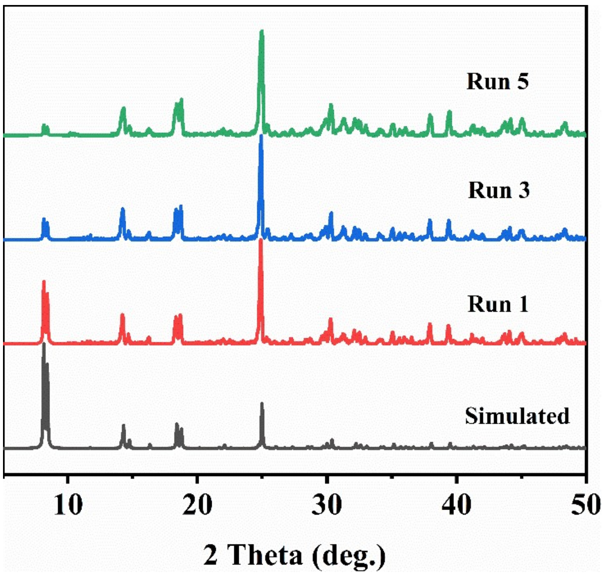

Fig. S5. PXRD spectra of **1'** after 5 runs of thioether oxidation.

Table S6 Control and condition optimization experiments of benzaldehyde silanization reaction catalyzed by **1'**

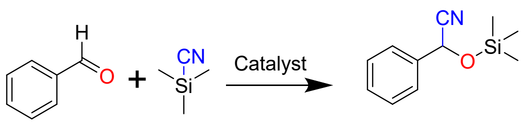

Entry	Catalyst (mg)	Time (h)	Temperature (°C)	Conv. (%)
1	0	3	30	11.21
2	10	3	30	36.32
3	20	3	30	58.71
4	30	3	30	92.67
5	40	3	30	99.16
6	50	3	30	98.21
7	40	3	20	69.34
8	40	3	10	45.11

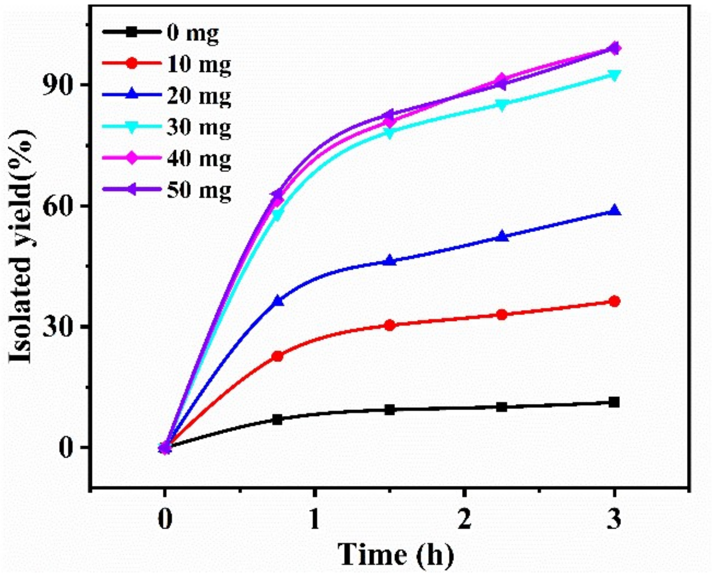

Fig. S6. Optimization of catalyst dosage for benzaldehyde silanization reaction

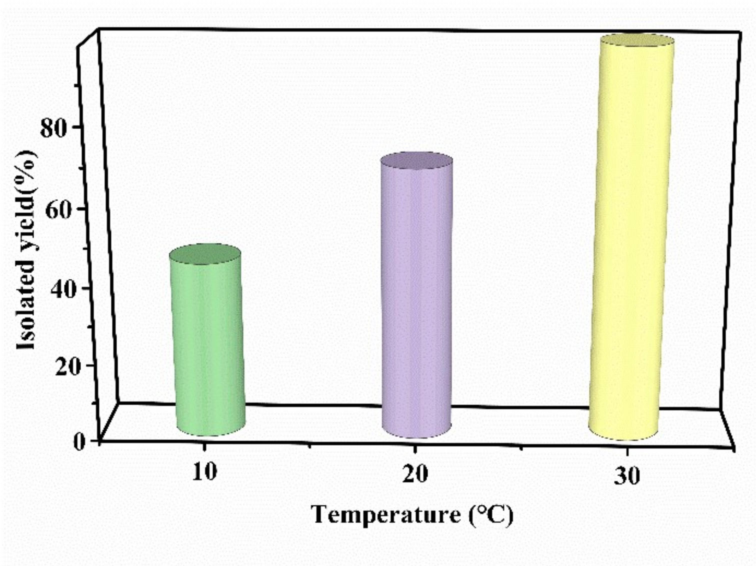

Fig. S7. The conversion of benzaldehyde silanization catalyzed by **1'** at different temperatures

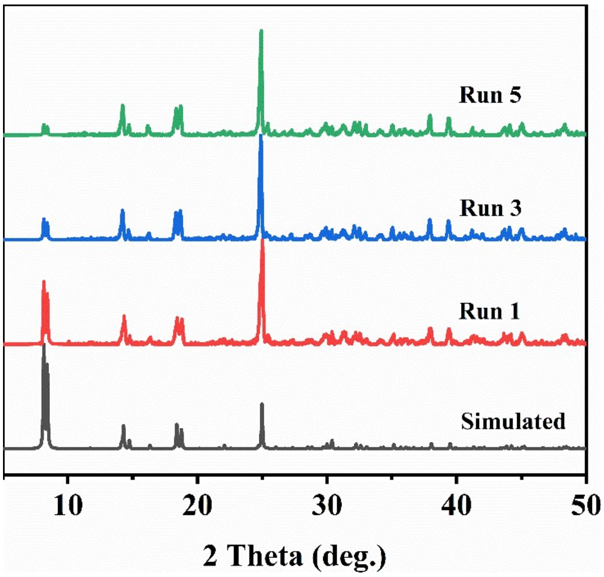

Fig. S8. PXRD spectrum of **1'** after 5 runs of catalytic silanization reaction.

Table S7 Control and condition optimization experiments of benzaldehyde Knoevenagel condensation reaction catalyzed by **1'**

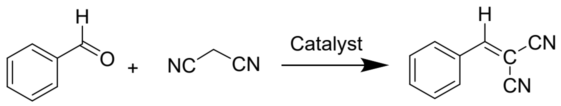

Entry	Catalyst (mg)	Time (h)	T (°C)	Conv. (%)
1	0	2	30	21.13
2	10	2	30	70.66
3	20	2	30	92.31
4	30	2	30	97.37
5	40	2	30	97.52
6	30	2	10	36.21
7	30	2	20	65.29
8	30	0.5	30	42.35
9	30	1	30	68.44
10	30	1.5	30	86.73
11	30	3	30	97.61
12	30	4	30	97.65

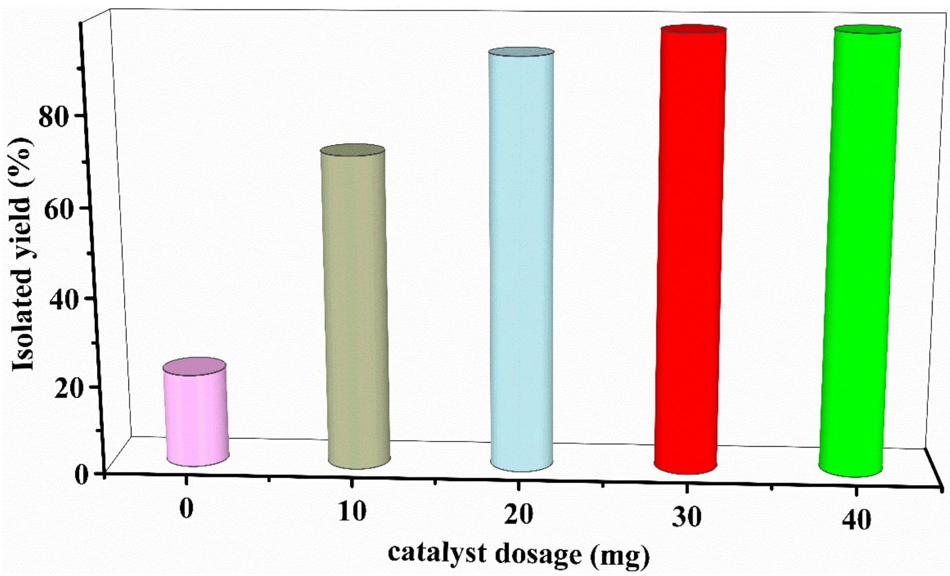

Fig. S9. The relationship between the amount of catalyst and the yield of catalytic conversion in benzaldehyde Knoevenagel condensation reaction.

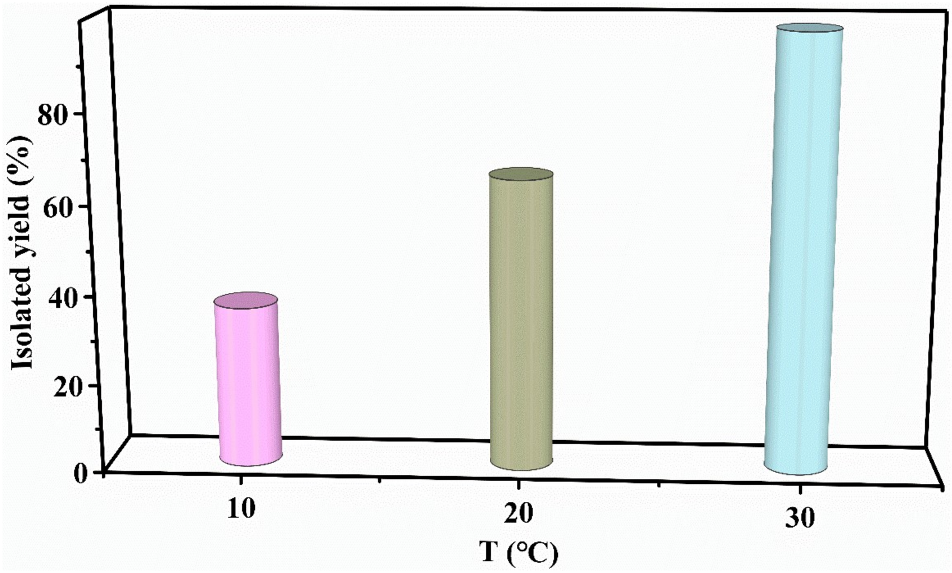

Fig. S10. The conversion of benzaldehyde Knoevenagel condensation reaction catalyzed by **1'** at different temperatures

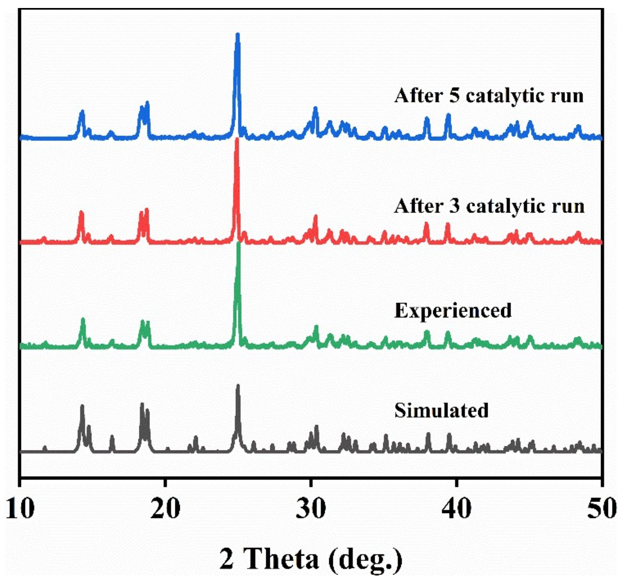

Fig. S11. PXRD spectrum of **1'** after 5 runs of catalytic Knoevenagel condensation reaction.

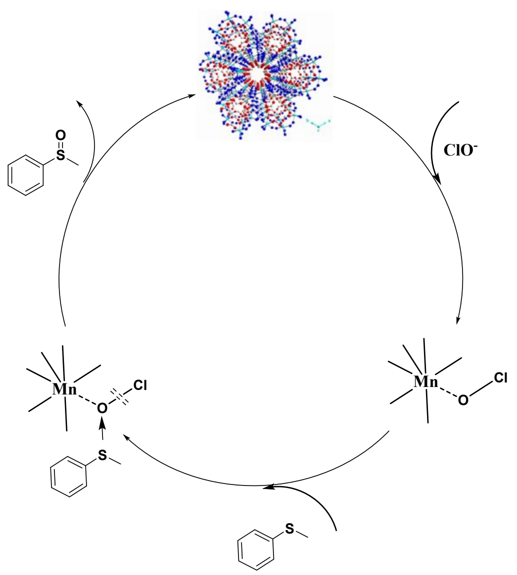

Fig. S12. Probable mechanism of the thioether oxidation reaction catalyzed by **1'**.

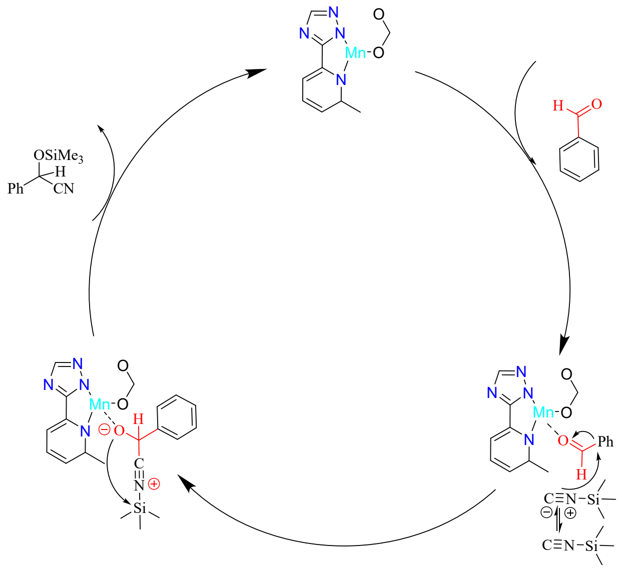

Fig. S13. Probable mechanism of the cyanosilylation reaction catalyzed by **1'**.

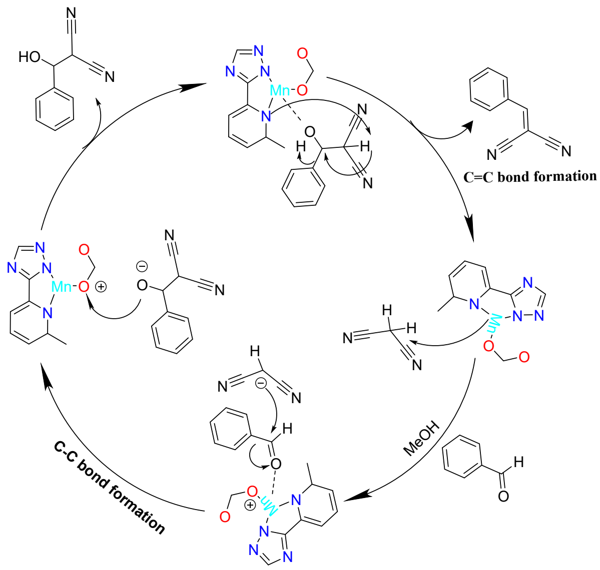

Fig. S14. Probable mechanism of the Knoevenagel condensation reaction catalyzed by **1'**.

Squeeze results for **1** is as follows:

```
loop_
  _platon_squeeze_void_nr
  _platon_squeeze_void_average_x
  _platon_squeeze_void_average_y
  _platon_squeeze_void_average_z
  _platon_squeeze_void_volume
  _platon_squeeze_void_count_electrons
  _platon_squeeze_void_content
   1  0.000  0.000  0.000         9         0 ' '
```

2	0.333	0.667	0.167	323	71 ' '
3	0.667	0.333	-0.167	322	70 ' '
4	0.000	0.000	0.500	320	70 ' '
5	0.667	0.333	0.333	11	0 ' '
6	0.333	0.667	0.667	11	0 ' '

That is, SQUEEZE gives 211 electrons/unit cell for the voids. If these electrons are all from CH_3OH ($16e^-$), each unit cell has 211/16 ≈ 13 CH_3OH molecules, and each formula unit has 1.5 CH_3OH molecules (since Z = 9). So the suitable formula for this compound should be **$\{[Mn_2(L)(HCOO)_2]\cdot 1.5CH_3OH\}_n$**

references

1. O. V. Zalomaeva, V. Y. Evtushok, I. D. Ivanchikova, T. S. Glazneva, Y. A. Chesalov, K. P. Larionov, I. Y. Skobelev and O. A. Kholdeeva, *Inorg. Chem.*, 2020, **59**, 10634-10649.

2. C. G. Werncke, C. Limberg, C. Knispel, R. Metzinger and B. Braun, *Chemistry – A European Journal*, 2011, **17**, 2931-2938.

3. Y. Zhang, W. D. Yu, F. Q. Wang, X. Wang, J. Zhou, C. Liu and J. Yan, *Chin. J. Chem* . 2024, **42**, 592-598.

4. X. Liu, N. Xu, X. Liu, Y. Guo and X. Wang, *Chem. Commun.*, 2022, **58**, 12236-12239.

5. O. V. Zalomaeva, N. V. Maksimchuk, G. M. Maksimov and O. A. Kholdeeva, *Eur. J. Inorg. Chem.*, 2018, **2019**, 410-416.

6. K. Lu, H. Qiu, X. Chen, T. Yuan, F. Xue and M. Ma, *J. Mol. Struct.*, 2024, **1295**, 136796.

7. P. Zhao, Y. Liu, C. He and C. Duan, *New J. Chem.*, 2023, **47**, 19114-19121

8. H. An, J. Zhang, S. Chang, Y. Hou and Q. Zhu, *Inorg. Chem.,* 2020, **59**, 10578-10590.

9. E. Echenique-Errandonea, M. E. López-Vargas, J. M. Pérez, S. Rojas, D. Choquesillo-Lazarte, J. M. Seco, I. Fernández and A. Rodríguez-Diéguez, *Catalysts*, 2022, **12**, 299.

10. A. Chanda and S. K. Mandal, *Inorg. Chem.,* 2024, **63**, 5598-5610.

11. Z. Arora, D. I. Eftemie, A. Spinciu, C. Maxim, A. M. Hanganu, M. Tudorache, B. Cojocaru, O. D. Pavel, P. Granger, M. Andruh and V. I. Pârvulescu, *ChemCatChem*, 2021, **13**, 4634-4644.

12. E. Zare and Z. Rafiee, *Appl. Organomet. Chem.*, 2020, **34**: e5516.

13. C. Guo, Y. Zhang, L. Zhang, Y. Zhang and J. Wang, *CrystEngComm*, 2018, **20**, 5327-5331.

14. K. Cai, W. Tan, N. Zhao and H. He, Cryst Growth Des., 2020, **20**, 4845-4851.

15. J. Qiao, B. Zhang, L. Zhang and Y. Liu, J. Mater. Chem. A, 2022, **10**, 17773-17781.

16. X. Zhang, X. Wang, C. Li, T. Hu and L. Fan, *J. Colloid Interface Sci.*, 2024, **656**, 127-136.